Equilibrium Transcytolemmal Water Exchange *in Vivo*

Charles S. Landis, Xin Li, Gabor Vetek, and Charles S. Springer

Chemistry Department, Brookhaven National Laboratory, Upton, New York 11973; and
Department of Chemistry, State University of New York, Stony Brook, New York 11794.

Introduction

It is commonly assumed that equilibrium transcytolemmal water exchange in tissue is sufficiently frequent as to be quite fast on any NMR time-scale that can be achieved with an extracellular contrast agent, CR, *in vivo*. A survey of literature values for cell membrane diffusional permeability coefficients, P, and cell sizes suggests that this should not be so (1) and quality data are becoming available that support this conclusion (1,2). We have assessed the effects of exchange in four different biological tissues: yeast cell suspensions, blood, rat brain gray matter, and rat thigh striated muscle, using these data. We show that, because of the exchange, the ^1H_2O longitudinal relaxation rate constant, R_1 ($=T_1^{-1}$), exhibits a non-linear dependence on the extracellular concentration of contrast reagent, $[CR_o]$. With the exception of blood, most tissues that have been studied depart the fast exchange *limit* (FXL) at $[CR_o]$ values below 100 μM. This has significant implications for the quantitative use of CRs as MRI tracers.

Theory

For the appraisal of the equilibrium exchange kinetics, we used a modification of the two-site exchange (2SX) model pioneered in McConnell's modifications of the Bloch Equations (1,2). The model uses seven parameters to describe how longitudinal relaxation is affected by transcytolemmal water exchange: R_{1o0} - extracellular R_1 in the absence of exchange and CR, R_{1i} - intracellular R_1 in the absence of exchange, r_{1o} - extracellular relaxivity, p_o, p_i - fractions of water outside and inside cells respectively, and τ_o, τ_i - mean residence times of water outside and inside cells, respectively. Only five of these are independent (1,2): τ_o and p_o are related to others by equilibrium mass balance [$\tau_o = \tau_i(1 - p_i)/p_i$; and $p_o = 1 - p_i$].

For evaluation of relaxation decay data with the 2SX model, one can hope to extract at most three observable quantities. This is because the model predicts that, under some conditions, the decay will be bi-exponential. For the recovery of longitudinal magnetization after inversion, this is expressed as the following,

$$M_z = M_0\{1 - 2[a_L\exp(-t_I R_{1L}) + a_S\exp(-t_I R_{1S})]\}$$

where M_z is the instantaneous magnetization, M_0 is its Boltzmann equilibrium value, a_L and R_{1L} are the fraction and rate constant for the *apparent* component with the larger T_1 (T_{1L}), a_S and R_{1S} are the fraction and rate constant for the *apparent* component with the smaller T_1 (T_{1S}), and t_I is the running time for recovery by relaxation. Since a_L and a_S are related ($a_S + a_L = 1$), there are only three independent quantities; R_{1L}, R_{1S}, and a_S (or a_L). These represent terribly complicated combinations of any five 2SX model parameters. We have provided such expressions (1).

Figure 1 is a "relaxivity plot" that shows the $[CR_o]$-dependencies of R_{1L} and R_{1S} in the 2SX model: for $R_{1i} = 0.67\ s^{-1}$, $R_{1o0} = 0.50\ s^{-1}$, and $r_{1o} = 3.75\ s^{-1}(mM)^{-1}$ (the value for GdDTPA^{2-} in cell-free (CF) saline at 4T) and p_o and τ_i values appropriate for skeletal muscle (SM) (1), **Table**. The extreme left hand side (LHS) of the plot represents the FXL if $(\tau_i^{-1} + \tau_o^{-1}) \gg |T_{1o0}^{-1} - T_{1i}^{-1}|$. Since the CR increases R_{1o} ($= r_{1o}[CR_o] + R_{1o0}$), moving from the LHS toward the right hand side (RHS) of the graph represents approaching the slow exchange regime (SXR). The CR•water binding equilibrium is very fast; τ_M^{-1} is approximately $10^9\ s^{-1}$ (1). We take the point at which $a_S/(a_S + a_L)$ becomes equal to $0.95 \cdot p_o$ (Fig. 2 and Table) to demarcate the slow exchange *limit* (SXL). After this, it is true that $(\tau_i^{-1} + \tau_o^{-1}) \ll |T_{1o}^{-1} - T_{1i}^{-1}|$, $R_{1S} = R_{1o} + \tau_o^{-1}$, $R_{1L} = R_{1i} + \tau_i^{-1}$, and the solid R_1 lines run parallel to their respective dashed (exchange-less) R_1 analogs. As one moves from the RHS toward the LHS, it is clear that R_{1S} and R_{1L} intend almost an "avoided crossing." However, before this happens, the intensity of the R_{1S} component vanishes (see Fig. 2). The *intermediate exchange* regime is not simply characterized, but we take the detectability of two populations ($a_S \approx 0.1$) to represent the border region between the SXR and FXR.

Tissue	p_o	τ_i (s)	$[CR_o]$ (mM) FXL/FXR	FXR/SXR	SXR/SXL
B	0.63	0.01	0.2	27.2	760
Y	0.65	0.70	0.1	0.4	9.7
SM	0.15	1.00	0.1	7.2	60
GM	0.30	0.60	0.1	1.8	55

Analysis

Figure 2 shows the $[CR_o]$-dependence of $a_S/(a_S + a_L)$ for SM, yeast (Y), brain grey matter (GM), and blood (B) tissue parameters (1), Table. **Figure 3** expands the region around the origin of Fig. 1 for the same four tissues and also gives the line for a CF saline solution. The p_o and τ_i values chosen for the Table have been determined experimentally (1-4). The three remaining 2SX parameters, R_{1i}, R_{1o0}, and r_{1o}, were held constant as given above.

Results gleaned from Figs. 2 and 3 are also summarized in the Table. The column labeled FXL/FXR indicates the $[CR_o]$ value above which each system can be thought to depart the FXL. This point can reasonably be taken as that at which the R_{1L} curve deviates from the r_{1CF} line when the abscissa is the *tissue* concentration, $[CR_t]$ ($\approx ([CR_o]p_o)/1.2$)) (1). The column labeled FXR/SXR indicates the $[CR_o]$ value when $a_S/(a_S + a_L)$ in Fig. 2 reaches 0.1. With good data, modern techniques can discriminate a small component contributing 10% (1-3). Finally, the column labeled SXR/SXL indicates the $[CR_o]$ value above which the system can be considered practically in the SXL ($a_S/(a_S + a_L) \approx 0.95p_o$). Although these latter values are high, it should be apparent from the FXL/FXR and FXR/SXR columns that the effects of exchange are significant even at very low $[CR_o]$ levels.

Discussion

From the general perspective, there are three important tissue compartmental water exchange equilibria to be considered: transendothelial exchange, transcytolemmal exchange in parenchyma, and transcytolemmal exchange in blood. In the earliest days of the use of CRs in MRI, it was usually assumed that each of these was in the FXL of any relevant NMR time-scale. This appeared to be a logical extension of results of the work on blood cell suspensions (1,4).

With further investigation, however, it became clear that it is quite easy (in fact, it is common) to achieve $[CR_p]$ levels of plasma-restricted agents such that transendothelial water exchange - that between the blood and parenchymal spaces - is definitely out of the fast exchange limit (1,2). The work presented here suggests that this can be true for compartmental exchange within the parenchyma as well.

The curves in Fig. 3 have considerable consequence. It is clear that R_{1L} deviates from the slope given by r_{1CF} at very small $[CR_o]$ values (<100 μM). Even if each curve is simply an empirical description of data (1), it could be used as a calibration curve for the $[CR_o]$-dependence of tissue ^1H_2O R_1. Often such a calibration is used to obtain [CR] values from measured R_1 values following a bolus injection of CR. Usually, a straight line with slope r_{1CF} is assumed. In other work, we have demonstrated the value of $[CR_o]$ usually rises well above 500 μM during such experiments (5). This suggests that the usage of a r_{1CF} calibration line for the analysis of bolus CR studies can lead to quite inaccurate results. It is also important to note that curves with the shape of those in Fig. 3 have been reported for *ex vivo* thigh and heart muscle preparations obtained after injection of CR into nephrectomized rats, with $[CR_t]$ serving as the abscissae (6). There is also evidence that r_{1o} can be quite sensitive to its environment; falling below (2) or rising above (3) its r_{1CF} value.

The most important message of the Table is that the exchange regime boundaries depend on all five 2SX parameters, not just τ_i, but particularly also on p_o. A significant consequence of this can be seen if the Y case is considered as a model for some tumor loci (1). Thus, for, say, a $[CR_o]$ value of 500 μM, tumor regions might be in the SXR while healthy GM regions within the same FOV might be in the FXR.

Acknowledgements

We thank the NIH (NIGMS) and DOE (OBER) for support for this work.

References

1) C.S. Landis, Xi Li, F.W. Telang, P.E. Molina, I. Palyka, G. Vetek, and C.S. Springer, *MRM*, submitted. **2)** C. Labadie, J-H. Lee, G. Vetek, and C. S. Springer,, *JMR B* **105**, 99-112 (1994). **3)** T.Q. Duong, C.S. Springer, C.H. Sotak, G.L. Bretthorst, G. Vetek, I. Palyka, J.J.H. Ackerman, and J.J. Neil, *PISMRM* **6**, 208 (1998). **4)** B. P. Hills and P. S. Belton, *Ann. Rpt. NMR Spectros.* **21**, 99-159 (1989). **5)** C.S. Landis, X. Li, G. Vetek, I. Palyka, F.W. Telang, P.E. Molina, and C.S. Springer, *PISMRM* **6**, 635 (1998). **6)** P. Wedeking, C. H. Sotak, J. Telser, K. Kumar, C. A. Chang, and M. F. Tweedle, *MRI* **10**, 97-108 (1992).

Figure 1

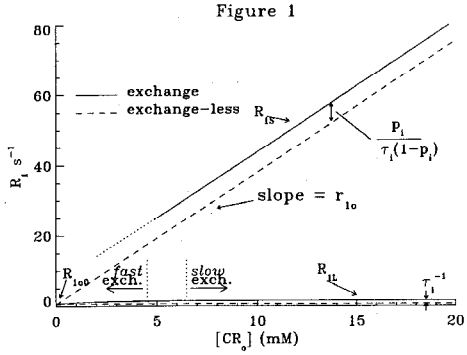

Figure 2

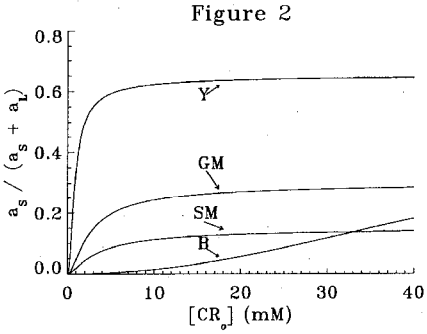

Figure 3